IRIS AperTO

UNIVERSITÀ DEGLI STUDI DI TORINO

AperTO - Archivio Istituzionale Open Access dell'Università di Torino

Doxorubicin-Loaded Nanobubbles Combined with Extracorporeal Shock Waves: Basis for a New Drug Delivery Tool in Anaplastic Thyroid Cancer

This is the author's manuscript

Original Citation:

Availability:

This version is available http://hdl.handle.net/2318/1563349 since 2016-05-30T08:39:11Z

Published version:

DOI:10.1089/thy.2015.0342

Terms of use:

Open Access

Anyone can freely access the full text of works made available as "Open Access". Works made available under a Creative Commons license can be used according to the terms and conditions of said license. Use of all other works requires consent of the right holder (author or publisher) if not exempted from copyright protection by the applicable law.

(Article begins on next page)

20 April 2024

IRIS AperTO

UNIVERSITÀ DEGLI STUDI DI TORINO

This is the author's final version of the contribution published as:

Marano, Francesca; Argenziano, Monica; Frairia, Roberto; Adamini, Aloe; Bosco, Ornella; Rinella, Letizia; Fortunati, Nicoletta; Cavalli, Roberta; Catalano, Maria Graziella. Doxorubicin-Loaded Nanobubbles Combined with Extracorporeal Shock Waves: Basis for a New Drug Delivery Tool in Anaplastic Thyroid Cancer. THYROID. 26 (5) pp: 705-16-716.
DOI: 10.1089/thy.2015.0342

The publisher's version is available at:
http://online.liebertpub.com/doi/10.1089/thy.2015.0342

When citing, please refer to the published version.

Link to this full text:
http://hdl.handle.net/2318/1563349

This full text was downloaded from iris - AperTO: https://iris.unito.it/

iris - AperTO

University of Turin's Institutional Research Information System and Open Access Institutional Repository

DOXORUBICIN-LOADED NANOBUBBLES COMBINED WITH EXTRACORPOREAL SHOCK WAVES: BASIS FOR A NEW DRUG DELIVERY TOOL IN ANAPLASTIC THYROID CANCER

Francesca Marano[1*], *MSc*, Monica Argenziano[2*], *PhD*, Roberto Frairia[1], *MD*, Aloe Adamini[1], *MSc*, Ornella Bosco[1], *PhD*, Letizia Rinella[1], *MSc*, Nicoletta Fortunati[3], *MD*, Roberta Cavalli[2], *PhD*, Maria Graziella Catalano[1], *MD, PhD*

[1]Department of Medical Sciences, University of Turin, Turin, Italy; [2]Department of Drug Science and Technology, University of Turin, Italy; [3]Oncological Endocrinology, AO Città della Salute e della Scienza di Torino, Turin, Italy.

*Both authors contributed equally to this work

Francesca Marano: francesca.marano@unito.it; Monica Argenziano: monica.argenziano@unito.it; Roberto Frairia: roberto.frairia@unito.it; Aloe Adamini: 329372@studenti.unito.it; Ornella Bosco: ornella.bosco@unito.it; Letizia Rinella: letizia.rinella@unito.it; Nicoletta Fortunati: nfortunati@cittadellasalute.to.it; Roberta Cavalli: roberta.cavalli@unito.it; Maria Graziella Catalano: mariagraziella.catalano@unito.it.

Running Title: Doxorubicin-loaded nanobubbles and ESWs for ATC

Keywords: Anaplastic thyroid cancer, Extracorporeal Shock Waves, nanobubbles, doxorubicin.

Corresponding Author: Maria Graziella Catalano, Department of Medical Sciences, University of Turin, Via Genova 3, 10126 Turin, Italy; tel. +39-0116705360; fax. +39-0116705366; mail: mariagraziella.catalano@unito.it

Abstract

Background: No standard chemotherapy is available for Anaplastic Thyroid Cancer (ATC). Drug-loaded nanobubbles (NBs) are promising innovative anti-cancer drug formulation; and, combining them with an externally applied trigger, may further control drug release at the target region. Extracorporeal Shock Waves (ESWs) are acoustic waves widely used in urology and orthopedics, with no side effects. The aim of the present work was to combine ESWs and new doxorubicin-loaded glycol chitosan NBs in order to target doxorubicin and enhance its anti-tumor effect in ATC cell lines.

Methods: CAL-62 and 8305C cells were treated with empty NBs, fluorescent NBs, free doxorubicin and doxorubicin-loaded NBs, in the presence or in the absence of ESWs. NB entrance was evaluated by fluorescence microscopy and flow cytofluorimetry. Cell viability was assessed by Trypan Blue exclusion and WST-1 proliferation assays. Doxorubicin intracellular content was measured by High Performance Liquid Chromatography.

Results: Treatment with empty NBs and ESWs, even in combination, was safe as cell viability and growth were not affected. Loading NBs with doxorubicin, and combining them with ESWs, generated the highest cytotoxic effect, resulting in drug GI_{50} reduction of about 40 %. Mechanistically, ESWs triggered intracellular drug release from NBs resulting in the highest nuclear drug content.

Conclusions: Combined treatment with doxorubicin-loaded NBs and ESWs is a promising drug delivery tool for ATC treatment with the possibility to use lower doxorubicin doses and thus limiting its systemic side effects.

INTRODUCTION

Anaplastic Thyroid Cancer (ATC) is one of the most lethal diseases with a median survival of only 5 months and a 1 year survival in less than 20% of patients (1,2). ATC may develop as a *de novo* tumor or can arise from a multi-step de-differentiation process of a pre-existing well differentiated papillary (PTC) or follicular (FTC) thyroid cancer. Of note, ATC frequently harbors mutations in the *BRAF* and *RAS* oncogenes observed in PTC and FTC (3,4). To date no standard therapy for ATC is available (5,6) and the recommended treatments, including surgery, radiotherapy and chemotherapy (7), fail to control local disease. Therefore, novel therapies are needed to improve disease outcomes (8,9). Extensive resection followed by adjuvant chemo-radiotherapy appears as the only treatment that modifies the survival of ATC patients (10,11). As far as chemotherapy is concerned, doxorubicin, the only agent approved as monotherapy by the FDA for ATC (12), has a response rate below 22% (13,14); moreover, if not specifically targeted to the tumor cells, doxorubicin affects also normal cells causing severe side effects, among which cardiotoxicity is the most prominent. Notably, the severity of these effects and their occurrence are dose dependent (15,16).

In order to find new therapeutic tools that allow reducing the cumulative dose, as well as to target the drug to the tumor site, nanoparticles encapsulating anticancer drugs appear to be promising delivery systems. In fact, they can carry loaded drugs to the tumor site through the blood stream taking advantage of the enhanced permeability and retention effect (EPR), due to the defective vascular architecture of the tumor tissue (17).

Recently, growing attention in the field of nanomedicine has been given to micro- and nanobubbles (NBs). NBs, composed of an external shell and a gas core, can deliver

diverse molecules, such as DNA and drugs, to target tissues in response to physical triggers, like ultrasound (US). US-induced drug delivery at specific sites is the result of bubble cavitation and increased cell permeability (18-23).

Extracorporeal Shock Waves (ESWs), acoustic waves widely used in urology for lithotripsy (24) since the 1980s, produce cavitation without heat induction. ESWs can be focused with high precision in depth and determine permeabilization of plasma membranes (25-27). We already reported elsewhere that ESWs increase paclitaxel-induced apoptosis in breast cancer cell lines (25), in anaplastic thyroid cancer cells (28), and in a Mat B-III rat syngeneic model of breast cancer (29). Furthermore, ESWs enhance the cytotoxic effect of doxorubicin and methotrexate in human osteosarcoma cell lines (30). Finally, ESW exposure has been shown to mediate DNA uptake into cells supporting *in vitro* transfection (27), and DNA-loaded microbubbles are associated with an increase in transgene expression in cultured cells exposed to ESWs (31). All these features make ESWs an ideal alternative to US in combination with drug-loaded NBs in delivery strategies.

Aim of this *in vitro* study was to combine the new doxorubicin-loaded glycol chitosan NBs and ESWs in order to enhance doxorubicin anti-tumor activity increasing intracellular drug release in ATC cells. The main goal is to provide the basis for future *in vivo* studies aiming at a new therapeutic approach for ATC patients.

MATERIALS AND METHODS

Materials

Ethanol (96%) was sourced from Carlo Erba (Milan, Italy). Epikuron 200® (soy lecithin containing 95% of dipalmitoyl phosphatidylcholine) was kindly gifted by Cargill (Hamburg, Germany). Doxorubicin hydrochloride was a kind gift from Pharmacia & Upjohn. 6-coumarin was purchased from Acros organics (Geel, Belgium). Ultrapure water was obtained using a 1-800 Millipore system (Molsheim, France). Penicillin and streptomycin were purchased from Gibco (Life Technologies Corp., Grand Island, NY, USA). DMEM-F12 medium was purchased from Invitrogen (Groningen, The Netherlands). RPMI 1640 and Fetal Calf Serum (FCS) were purchased from Euroclone (Wetherby, West York, UK). Phenylmethylsulfonyl Fluoride (PMSF) and WST-1 cell proliferation reagent were purchased from Roche Diagnostics Corporation (Indianopolis, IN, USA). Penicillin, streptomycin, non-essential amino acids (NEAA), palmitic acid, perfluoropentane, glycol chitosan (Mw = 68 kDa), fluorescein isothiocyanate (FITC), Nonidet 40 (NP40), desoxycholate sodium, sodium dodecyl sulphate (SDS), phosphate buffered saline (PBS), aprotinin, sodium orthovanadate, 4-(2-Hydroxyethyl) piperazine-1-ethanesulfonic acid (Hepes), sodium carbonate (Na_2CO_3), magnesium chloride ($MgCl_2$), potassium chloride (KCl), sodium chloride (NaCl), 1,4-dithiothreitol (DTT), Triton X-100, glycerol, and ethylenediaminetetraacetic acid (EDTA) were all purchased from Sigma-Aldrich (St Louis, MO).

Preparation of NBs

NBs were formulated by purposely tuning the method previously reported (18) using perfluoropentane as inner core component and glycol chitosan for the shell. Firstly, an ethanolic solution containing palmitic acid and Epikuron 200® (1% w/v) was added to

perfluoropentane, to form a pre-emulsion. After the addition of ultrapure water the system was homogenized using a high shear homogenizer (Ultraturrax®, IKA, Königswinter, Germany) in an ice-bath. Then, to obtain the polymeric NBs, an aqueous solution of the glycol chitosan polymer (2.7 % w/v, pH 5) was drop-wise added under mild magnetic stirring.

Doxorubicin as base was obtained adding a saturated solution of Na_2CO_3 (1.4 g/ml) to a doxorubicin HCl solution in deionized water (200 mg/ml) drop by drop. To obtain the drug-loaded NBs a pre-emulsion was obtained by adding an Epikuron® 200 and palmitic acid ethanolic solution (1% w/v) containing doxorubicin base to perfluoropentane under magnetic stirring. After the addition of ultrapure water, the system was homogenized using a high shear homogenizer. To obtain the NBs, an aqueous glycol chitosan solution (2.7 % w/v, pH 5) was drop-wise added under magnetic stirring. A purification step by dialysis was then carried out to eliminate the potential free drug.

Two types of fluorescent glycol chitosan NBs were prepared. Empty fluorescent NBs were obtained by adding 6-coumarin to the perfluoropentane core. FITC-labelled doxorubicin-loaded NBs were prepared by inserting the green fluorescent FITC in the NB shell, in order to have a double labeling, exploiting the intrinsic fluorescence of doxorubicin. For this purpose, an amount of FITC (0.02 % w/v) was added to the pre-formed doxorubicin-loaded NB suspension and incubated under stirring for 24 hours in the dark at room temperature.

Characterization and stability of NBs

The average diameter and polydispersity index of NB formulations were determined by photon correlation spectroscopy (PCS); the zeta potential was determined by

electrophoretic mobility using a 90 Plus instrument (Brookhaven, NY, USA). The analyses were performed at a scattering angle of 90° at a temperature of 25° C, using NB suspension diluted with deionized distilled water. For zeta potential determination, samples of diluted NB formulations were placed in the electrophoretic cell, where an electric field of approximately 15 V/cm was applied.

The morphology of formulations was evaluated by Transmission Electron Microscopy (TEM), using a Philips CM10 instrument (Eindhoven, NL).

***In vitro* doxorubicin release kinetics**

In vitro release studies were carried out using a multi-compartment rotating cell. The donor compartment containing 1 ml of doxorubicin-loaded glycol chitosan NB suspension or doxorubicin hydrochloride aqueous solution as control was separated by a dialysis membrane (Spectrapore, cut-off 12000-14000 Da) from a receiving compartment, containing saline phosphate buffer at pH 7.4. At fixed times the receiving phase was withdrawn and replaced with fresh receiving medium. The doxorubicin content was determined by a High Performance Liquid Chromatography (HPLC) system consisting of a pump (LC-9A PUMP C, Shimadzu, Japan) equipped with a fluorescence detector (Chrompack, Japan). Analyses were performed using an Agilent TC C_{18} column (250 mm × 4.6 mm, 5 µm). The external standard method was used to calculate the drug concentration. For this purpose, 1 mg of doxorubicin was weighed, placed in a volumetric flask, and dissolved in water to obtain a stock standard solution. This solution was then diluted using the mobile phase, providing a series of calibration solutions, subsequently injected into the HPLC system.

Moreover, *in vitro* release kinetics of doxorubicin from doxorubicin-loaded glycol chitosan NBs were investigated after ESW treatment. 1 ml of doxorubicin-loaded NBs

were placed in 20 mm polypropylene tubes (Nunc, Wiesbaden, Germany) and treated with ESWs (0.59 mJ/mm^2, 500 pulses).

Cell lines and culture conditions

ATC cell lines, CAL-62 and 8305C, were purchased from Deutsche Sammlung von Mikroorganismen and Zellkulturen (Braunschweig, Germany), which certifies the origin and identity of the cells. The rat embryonic cardiomyocyte cell line, H9C2, was purchased from ATCC (Manassas, Virginia, USA). Cells were routinely maintained in 75 cm^2 flasks at 37°C, in 5% CO_2 and 95% humidity, with 100 IU/ml penicillin and 100 μg/ml streptomycin added in DMEM-F12 for CAL-62 and H9C2 cells, or RPMI 1640 plus 1% NEAA for 8305C cells, supplemented with 10% FCS.

ESW treatment

The shock wave generator utilized for the *in vitro* experiments is a piezoelectric device (Piezoson 100, Richard Wolf, Knittlingen, Germany) designed for clinical use in orthopedics and traumatology. The experimental set-up has been reported elsewhere (25). Aliquots of 1 ml of cell suspension adjusted to 1 x 10^6 cells/ml were placed in 20 mm polypropylene tubes, completely filled with culture medium. Subsequently, cells were gently pelleted by centrifugation at 250 x *g* in order to minimize motion during shock wave treatment. Each cell-containing tube was placed in vertical alignment with the focal area and was adjusted so that the central point of the focal area corresponded to the centre of the tube bottom. The shock wave unit was kept in contact with the cell containing tube by means of a water-filled cushion. Common ultrasound gel was used as a contact medium between cushion and tube. ESW treatment was as follows: energy flux density (EFD) = 0.59 mJ/mm^2, 500 pulses (frequency = 4 shocks/s), peak positive

pressure 64 MPa, peak negative pressure 12 MPa. After treatment, cell viability was evaluated in a hemocytometer chamber by a Trypan Blue dye exclusion assay.

Cell viability assay

CAL-62 and 8305C cells were treated with ESWs; empty NBs (0.9-5.4 x 10^6 NBs/ml); free doxorubicin (0.25-3 μM); doxorubicin-loaded NBs (0.25-3 μM); empty NBs + ESWs; doxorubicin + ESWs; doxorubicin-loaded NBs + ESWs; empty NBs + free doxorubicin + ESWs. H9C2 cells were treated with empty NBs (0.9-5.4 x 10^6 NBs/ml); free doxorubicin (0.25-3 μM); doxorubicin-loaded NBs (0.25-3 μM). Cells in maintenance medium plus 1% FCS were used as controls (Basal). After different treatments, cells were seeded at 3 x 10^3 cells/well in 96-well plates (Corning, New York, NY, USA). After 24 hours, drug containing medium was replaced with maintenance medium plus 1% FCS. Viable cells were determined at different times using the Cell Proliferation Reagent WST-1, following the manufacturer's instructions. This is a colorimetric assay for the quantification of cell viability and proliferation, based on the cleavage of the tetrazolium salt WST-1 by mitochondrial dehydrogenases. Briefly, 10 μl of WST-1 were added to each well. After 1 hour incubation, absorbance at 450 nm was measured using a plate reader (Model 680 Microplate Reader, Bio-Rad, Hercules, CA, USA). Four replicate wells were used to determine each data point. Growth inhibition fifty (GI_{50}), corresponding to the concentration of the compound that inhibits 50% cell growth, was calculated.

NB internalization

Cells were seeded at 5 x 10^5 cells/well in 6-well plates (Corning, New York, NY, USA) and treated with 6-coumarin-labeled glycol chitosan NBs (0.9-5.4 x 10^6 NBs/ml). After 24 hours, green fluorescence in the cells was assessed by flow cytometer (EPICS XL, Coulter Corp., Hialeah, FL). Ten thousand events were acquired for each sample.

To evaluate NB entrance, cells were seeded at 3 x 10^3 cells/well in 96-well plates and treated with 6-coumarin-labeled glycol chitosan NBs at 0.9 and 1.8 x 10^6 NBs/ml. After 24 hours, cells were observed with an inverted fluorescence microscope Leica DMI 4000 B (Leica Microsystems, Wetzlar, Germany) and photos were taken with a Leica DCF340 FX digital camera system (Leica Microsystems., Wetzlar, Germany) at x 200 and x 400 magnifications.

To study the ESW effects on NBs, cells were treated with 1 μM doxorubicin-loaded FITC-NBs in the presence or absence of ESWs. 1 hour after ESW treatment, cells were cytospun on slices and observed with an inverted fluorescence microscope Leica DMI 4000 B. Photos of single channels and overlayers were taken with a Leica DCF340 FX digital camera system at x 200 final magnification.

Cell drug uptake

Cell drug uptake was investigated by the quantitative evaluation of intracellular doxorubicin accumulation. CAL-62 and 8305C cells were treated with 1 μM free doxorubicin or doxorubicin-loaded glycol chitosan NBs in the presence or in the absence of ESW treatment and seeded at 5 x 10^6 cells/well in 6-well plates (Corning, New York, NY, USA).

After treatment for 24 hours, whole cell lysates were prepared in RIPA buffer (1% NP40, 0.5% desoxycholate sodium, 0.1% SDS in PBS pH 7.4, with 10 mg/ml PMSF,

30μl/ml aprotinin and 100 mM sodium orthovanadate) and incubated on ice for 30 min; cells were then centrifuged for 20 min at 15,000 x *g* at 4°C, and clear supernatants were used.

Nuclear extracts were obtained in hypotonic buffer (10 mM Hepes, 1.5 mM $MgCl_2$, 10 mM KCl, 0,5 mM DTT, 1 mM PMSF, pH 7.9), added with Triton X-100 (0.1% final concentration) and incubated for 15 min on ice. Cells were then disrupted by repeated passages into a syringe. Nuclear pellets, obtained by centrifugation at 11,000 × *g* for 20 min, were rinsed once in hypotonic buffer, resuspended in hypertonic buffer (20 mM Hepes, 1.5 mM $MgCl_2$, 25% (v/v) glycerol, 420 mM NaCl, 0.5 mM DTT, 1 mM PSMF, 0.2 mM EDTA, pH 7.9), gently shacked for 30 min at 4 °C and then centrifuged at 15,000 × *g* for 10 min. The final supernatants were used. After dilution with the mobile phase, the samples were stirred for 2 min, and injected into the HPLC system, for the quantitative determination of doxorubicin. Cell uptake was expressed as ng of doxorubicin/10^6 cells.

Statistical Analysis

Data are expressed throughout the text as means ± SD, calculated from at least three different experiments. Comparison between groups was performed with analysis of variance (two-way ANOVA) and the threshold of significance was calculated with the Bonferroni test. Comparison between ESW-treated cells and no ESW-treated cells was performed with t-test. Statistical significance was set at $p<0.05$.

RESULTS

Characterization of new doxorubicin-loaded glycol chitosan NBs

The average diameter, polydispersity index (PDI) and zeta potential values of the NBs, before and after loading with doxorubicin, determined at 25 °C, are reported in Table 1. Empty NBs showed an average diameter lower than 500 nm and a positive surface charge. Doxorubicin loading did not significantly alter these values, nor fluorescent labeling (data not shown). A TEM image of doxorubicin-loaded glycol chitosan NBs is shown in Fig. 1A. The NBs showed a spherical shape, smooth surface and a well-defined core-shell structure, with a polymeric shell thickness of about 40 nm.

Fig. 1B shows the *in vitro* release profile of doxorubicin from NBs in phosphate buffer (pH 7.4) in the presence or absence of ESW treatment compared to a doxorubicin hydrochloride aqueous solution, used in therapy. After 3 hours, only 9.2 % of the drug was released in the absence of ESW with respect to 40.3% of free doxorubicin ($p<0.001$); moreover, no initial burst effect was observed showing NB stability. Interestingly, doxorubicin was released to a larger extent following ESW treatment with 500 pulses at 0.59 mJ/mm^2. Particularly, after 3 hours, ESWs generated an increase of about 70% of released doxorubicin with respect to NBs without ESW treatment ($p<0.001$).

Safety of ESW treatment and empty NBs

In a preliminary series of experiments, cells were treated with different numbers of pulses (from 100 to 2000 at EFD = 0.59 mJ/mm^2), in order to find the best treatment in terms of cell viability and growth. The used energy was within the range of clinical use; in ESW therapy; shock waves are applied ranging from 0.01 to 0.6 mJ/mm^2 (32). Soon after treatment with 500 pulses, cell viability in both CAL-62 and 8305C cell lines was

higher than 87 % (data not shown). Moreover, the same treatment did not affect cell growth of both cell lines up to 72 hours (Fig. 2A and 2B). Therefore, this treatment schedule was chosen for further experiments.

As the shell influences NB characteristics and behavior, we tested whether empty NBs affected cell viability of both ATC cell lines. Glycol chitosan NBs had no significant effect on cell viability of both cell lines (Fig. 2C and 2D). Moreover, as shown in Fig. 2E and 2F, empty NBs had no significant effect on cell growth even when used in combination with ESWs and this allowed us to exclude any non-specific effect of the combined treatment on cell viability. In both ATC cell lines, glycol chitosan NBs entered the cells in a dose-dependent manner, as shown in Fig. 3A and 3B, and were visible inside the cells (Fig. 3C and 3D).

Cytotoxicity of doxorubicin-loaded glycol chitosan NBs combined with ESWs

As shown in Fig. 4A and 4B, free doxorubicin had cytotoxic effect in both ATC cell lines only at levels hardly obtainable in patients receiving the doxorubicin dose of 60 mg/m^2 (33) with a GI_{50} at 48 hours of 1.57 μM in CAL-62 and 3.93 μM in 8305C cells, respectively (Table 2). ESW treatment increased the cytotoxic effect of the free drug (Fig. 4C and 4D). In fact, the GI_{50} decreased to 1.33 μM in CAL-62 ($p<0.05$) and to 3.17 μM in 8305C cells ($p<0.05$) (Table 2). Drug-loaded NBs, even without ESWs, were more effective in inducing cytotoxicity in both cell lines with respect to free doxorubicin (Fig. 4E and 4F). In fact, as reported in Table 2, the GI_{50} decreased to 1.13 μM in CAL-62 ($p<0.001$) and to 2.98 μM in 8305C cells ($p<0.05$). The combination of ESWs with doxorubicin-loaded NBs had the greatest cytotoxic effect (Fig. 4G and 4H) with a GI_{50} of 0.95 μM in CAL-62 ($p<0.001$) and 2.12 μM in 8305C ($p<0.001$), respectively (Table 2). In a second series of experiments, the cytotoxicity of CAL-62

treated with empty NBs in combination with free doxorubicin and ESWs was evaluated. This treatment was more cytotoxic with respect to the free drug alone; in fact, the GI_{50} decreased to 1.26 μM ($p<0.01$) (Table 2). However, combining ESWs with free doxorubicin plus empty NBs was less effective than using ESWs with doxorubicin loaded into NBs.

Effect of empty NBs and doxorubicin-loaded NBs on rat cardiomyocytes

Empty NBs were found to be safe in rat cardiomyocytes H9C2 cells (Fig. 5A) and they entered the cells at a level comparable to that observed for cancer cells (Fig. 5B). In these cells, drug-loaded NBs did not increase the cytotoxic effects of doxorubicin (Fig. 5C and 5D) with a GI_{50} at 48 hours of 1.75 μM and 1.68 μM for doxorubicin-loaded NBs and free doxorubicin, respectively.

ESW effects on intracellular doxorubicin release and content

To get insight into the mechanisms of ESW action on NB drug delivery, cells were treated with FITC-labeled doxorubicin-loaded glycol chitosan NBs, either in the presence or in the absence of ESWs. In the cells treated with NBs alone, we observed the co-localization of the two fluorescent molecules (FITC and doxorubicin), indicating no perturbation of the NB structure after internalization into the cells (Fig. 6, panels c and c'). In contrast, in the cells that received the combined treatment (NBs plus ESWs), there was a loss of co-localization of the two molecules (Fig. 6, panels f and f').

Finally, the intracellular doxorubicin content was investigated after ESW treatment. As shown in Fig. 7A, ESWs increased the concentration of intracellular free doxorubicin from 0.3 to 1.8 ng /10^6 cells ($p<0.01$); a further increase to 17.2 ng /10^6 cells ($p<0.001$) was obtained when the drug was loaded within NBs, but it was the combined treatment

that showed the best effect with a doxorubicin concentration in the cell lysate of about 30 ng/10^6 cells ($p<0.001$).

As shown in Fig. 7B, NB formulations greatly increased the nuclear amount of doxorubicin to 15.2 ng /10^6 cells with respect to 0.2 ng /10^6 cells of the free drug ($p<0.001$); but, again, the highest nuclear drug concentration was obtained after the combined treatment with ESWs and doxorubicin-loaded NBs (26.2 ng/10^6 cells, $p<0.001$). As consequence, doxorubicin accumulated into the nuclei, its site of action, resulting in cell death.

DISCUSSION

The present study demonstrates, for the first time, that the combined treatment with doxorubicin-loaded glycol chitosan NBs and ESWs enhances cytotoxicity of doxorubicin in ATC cells.

As a curative therapy for ATC has not been identified yet (5,6), it is mandatory to better characterize the mutational landscape of ATC in order to identify new possible candidates for targeted therapy (34,35), and to search novel therapies against this fatal disease. Unfortunately, to date different targeted therapies used in ATC, have not shown any success and others, demonstrating a potential effectiveness, have not reached a clinical setting. Thyroidectomy with neoadjuvant PLX4720, an inhibitor of *B-RAF*^{V600E}, was effective in an ATC *B-RAF*^{V600E} orthotopic mouse model (36). The treatment of an ATC mouse model overexpressing FOXM1 (Forhead Box Protein M1) with thiostrepton, a compound that reduces FOXM1 activity (37,38), strongly reduced tumor burden and abolished metastasis (39). LBH589, a potent pan-deacetylase inhibitor with anticancer activity showed potent cytotoxic and anti-invasive activities in both *in vitro* and *in vivo* models of ATC (40,41) and conferred radioiodine sensitivity to ATC cell lines and primary cultures (42).

Doxorubicin is the only chemotherapeutical drug approved by the FDA for ATC treatment in monotherapy (12), but it has a poor clinical response (13,14), and extremely severe side effects (15,16,43). Therefore, targeting doxorubicin to the tumor cells, increasing its cytotoxicity while reducing side effects, could be an important goal in ATC therapy.

In this work, new glycol chitosan-shelled NBs were designed for the delivery of doxorubicin. Chitosan derivatives are attractive excipients for their excellent

biocompatibility, biodegradability, and low immunogenicity. Glycol chitosan was already used with promising results in many studies for drug targeting and delivery. Previous i*n vivo* studies reported very low systemic toxicity for different glycol chitosan nanoparticles and their preferential tumor localization in tumor-bearing animals (44-48). NBs filled with perfluorocarbon have been already used for contrast agent preparation because of their stability and biological inertness. Moreover, the very low water solubility, that reduces the gas dissolution rate from the NB inner core into the bloodstream, stabilizes the system and increases the *in vivo* lifetime of the bubbles. As described elsewhere, perfluoropentane cored and chitosan shelled NBs have recently been designed as theranostic agents (49).

Safety testing of unloaded NBs was fundamental in order to exclude any undesired effect of the shell. In our study, empty glycol chitosan NBs entered CAL-62 and 8305C cells and had no effect on cell viability of both the ATC cell lines, thus they appear to be safe even when used in combination with ESWs. Once glycol chitosan NB safety was proven, we demonstrated that doxorubicin-loaded NBs generated a higher cytotoxic effect compared to the free drug. Even if increased doxorubicin cytotoxic effects have been reported for drug combinations with either PXD101 (50) or valproic acid (51) histone deacetylase inhibitors, to date, no other study has used delivery systems to target doxorubicin in ATC. Nevertheless, the cytotoxic efficacy of other types of nanoparticles to deliver doxorubicin has been reported in other tumor models. For instance, polylactide-graft-doxorubicin nanoparticles with pH-triggered drug delivery exhibited higher efficacy in killing MCF-7 breast cancer cells (52) and doxorubicin-loaded glucan nanoparticles decorated with trastuzumab antibodies (against HER2) were more efficient in reducing tumor volume in an *in vivo* murine breast cancer HER2 positive

model (53) compared to free doxorubicin. Yu J. *et al*. (54) reported that folic acid-conjugated glycol chitosan nanoparticles have a great cytotoxicity against folate receptor-positive HeLa cervical cancer cells and other authors (55) demonstrated that doxorubicin-loaded apotransferrin and lactoferrin nanoparticles were more cytotoxic than the free drug in an *in vivo* rat hepatocellular carcinoma model.

The novelty of our work is the use of ESWs as physical strategy to trigger drug release from NBs specifically at the tumor site. We report here that ESWs enhanced *in vitro* doxorubicin-loaded NB cytotoxicity, decreasing the drug GI_{50} of 40 % in CAL-62 and 46 % in 8305C cells, respectively. The reduction of the GI_{50} is notable, since the use of lower doses of doxorubicin is essential to reduce its side effects (56). Moreover, we observed an increased cytotoxic effect even when we used the ESWs in combination with the free doxorubicin formulation either in the absence (free doxorubicin plus ESWs) or in the presence of empty NBs (free doxorubicin plus empty NBs and ESWs). All these effects may be the consequences of cavitation which occurs when acoustic waves propagate into fluids. In fact, cavitation might determine both the perturbation of the NBs, resulting in the drug release, as well as the transient permeabilization of both plasma and nuclear membranes, thus allowing drug penetration into the cell. It has already been reported that ESWs increase cell permeability (26-28), affecting drug efficacy in breast cancer cells (25), in anaplastic thyroid cancer cells (28), and in an *in vivo* breast cancer model (29). However, the greatest effect was obtained with doxorubicin-loaded NBs used in combination with ESWs.

As far as the mechanism of action of the combined treatment (doxorubicin-loaded NBs and ESWs) is concerned, ESWs increased the intracellular doxorubicin release from NBs, and, as a consequence, the drug accumulated in the nuclei, where doxorubicin

intercalates into DNA and inhibits topoisomerase II, resulting in DNA damage and cell death (57). As nuclear localization is considered a mechanism to overcome drug resistance (58,59), combining ESWs and drug-loaded NBs may be also viewed as a new therapeutic approach to circumvent cellular drug resistance.

All these observations explain the enhanced cytotoxic effects of the combined treatment allowing insights into its mechanism of action. We suggest that: 1. NBs act as stable doxorubicin reservoir in the thyroid cancer cells with prolonged drug release 2. ESWs further increase doxorubicin release from NBs leading to a higher intracellular drug content and favoring its nuclear accumulation.

The cytotoxic effects of doxorubicin-loaded NBs and ESWs, that will allow using lower doses, altogether with the EPR effect, will reduce the exposure of non-target organs to doxorubicin. However, as expected, our *in vitro* experiments on rat cardiomyocytes H9C2 did not show any significant difference between free doxorubicin and doxorubicin loaded into NBs, but they cannot completely predict the *in vivo* toxicity on off-target tissues. Only further *in vivo* experiments will ultimately define the ability of this combined treatment in limiting the systemic side-effects of the drug, and in the enhancement of its efficacy. Many authors have already reported a higher concentration of doxorubicin in tumors of animals treated with doxorubicin-loaded nanocarriers compared to those treated with the free drug (60-62), but to date nobody has used ESWs to trigger drug release. The ESW generator can be easily placed in contact with a water-based gel on the skin and ESWs can be focused at the tumor site, thus potentially permitting to target specific ATC lesions. Finally, unlike US, ESWs have not heating effects. This could be an advantage for *in vivo* application since temperature elevation is

difficult to control spatially and temporally, especially in large tumors with heterogeneous vascularization, such as ATC (63).

In conclusion, this first *in vitro* study on the use of ESWs and doxorubicin-loaded NBs, suggests that this combined treatment may be a promising drug delivery tool for targeted ATC treatment, but this approach now needs further characterization *in vivo* in preclinical models.

ACKNOWLEDGEMENTS

We thank: Sebastiano Colombatto, Department of Oncology, University of Turin, Turin, Italy. We thank Med & Sport 2000 S.r.l., Turin, Italy, for providing the shock wave generator. The study was supported by Fondazione CRT Turin, Italy, to Maria Graziella Catalano; by "Progetto Ateneo 2011'', University of Turin, Turin, to Roberto Frairia; and by "Research Fund ex-60%", University of Turin, Turin, to Roberta Cavalli.

AUTHOR DISCLOSURE STATEMENT

No competing financial interests exist.

REFERENCES

1. Nagaiah G, Hossain A, Mooney CJ, Parmentier J, Remick SC 2011 Anaplastic thyroid cancer: a review of epidemiology pathogenesis and treatment. J Oncol **2011:**542358.

2. Smallridge RC, Copland JA 2010 Anaplastic thyroid carcinoma: pathogenesis and emerging therapies. Clin Oncol **22:**486-497.

3. Guerra A, Di Crescenzo V, Garzi A, Cinelli M, Carlomagno C, Tonacchera M, Zeppa P, Vitale M 2013 Genetic mutations in the treatment of anaplastic thyroid cancer: a systematic review. BMC Surg **13:**S44.

4. Nikiforov YE 2004 Genetic alterations involved in the transition from well-differentiated to poorly differentiated and anaplastic thyroid carcinomas. Endocr. Pathol **15:**319-327.

5. Neff RL, Farrar WB, Kloos RT, Burman KD 2008 Anaplastic thyroid cancer. Endocrinol Metab Clin North Am **37:**525-538.

6. Wein RO, Weber RS 2011 Anaplastic thyroid carcinoma: palliation or treatment? Curr Opin Otolaryngol Head Neck Surg. **19:**113-118.

7. Smallridge RC, Ain KB, Asa SL, Bible KC, Brierley JD, Burman KD, Kebebew E, Lee NY, Nikiforov YE, Rosenthal MS, Shah MH, Shaha AR, Tuttle RM; American Thyroid Association Anaplastic Thyroid Cancer Guidelines Taskforce 2012 American Thyroid Association guidelines for management of patients with anaplastic thyroid cancer. Thyroid **22**:1104-1039.

8. Catalano MG, Poli R, Pugliese M, Fortunati N, Boccuzzi G 2010 Emerging molecular therapies of advanced thyroid cancer. Mol Aspects Med **31:**215-226.

9. Catalano MG, Fortunati N, Boccuzzi G 2012 Epigenetics modifications and therapeutic prospects in human thyroid cancer. Front Endocrinol (Lausanne) **19:**3-40.

10. Brignardello E**,** Gallo M, Baldi I, Palestini N, Piovesan A, Grossi E, Ciccone G, Boccuzzi G 2007 Anaplastic thyroid carcinoma: clinical outcome of 30 consecutive patients referred to a single institution in the past 5 years. Eur J Endocrinol **156:**425-430.

11. Brignardello E, Palestini N, Felicetti F, Castiglione A, Piovesan A, Gallo M, Freddi M, Ricardi U, Gasparri G, Ciccone G, Arvat E, Boccuzzi G 2014 Early surgery and survival of patients with anaplastic thyroid carcinoma: analysis of a case series referred to a single institution between 1999 and 2012. Thyroid **24:**1600-1606.

12. Haddad RI, Lydiatt WM, Ball DW, Busaidy NL, Byrd D, Callender G, Dickson P, Duh QY, Ehya H, Haymart M, Hoh C, Hunt JP, Iagaru A, Kandeel F, Kopp P, Lamonica DM, McCaffrey JC, Moley JF, Parks L, Raeburn CD, Ridge JA, Ringel MD, Scheri RP, Shah JP, Smallridge RC, Sturgeon C, Wang TN, Wirth LJ, Hoffmann KG, Hughes MJ 2015 Anaplastic Thyroid Carcinoma, Version 2.2015. Natl Compr Canc Netw **13:**1140-1150.

13. Giuffrida D, Gharib H 2000 Anaplastic thyroid carcinoma: current diagnosis and treatment. Ann Oncol **11:**1083-1089.

14. Haigh PI 2000 Anaplastic thyroid carcinoma. Curr Treat Options Oncol **1:**353-357.

15. Carvalho C, Santos RX, Cardoso S, Correia S, Oliveira PJ, Santos MS, Moreira PI 2009 Doxorubicin: the good the bad and the ugly effect. Curr Med Chem **16:**3267-3285.

16. Chatterjee K, Zhang J, Honbo N, Karliner JS 2010 Doxorubicin cardiomyopathy. Cardiology **115:**155-162.

17. Maeda H 2010 Tumor-selective delivery of macromolecular drugs via the EPR effect: background and future prospects Bioconjug Chem **21:**797-802.

18. Cavalli R, Bisazza A, Trotta M, Argenziano M, Civra A, Donalisio M, Lembo D 2012 New chitosan nanobubbles for ultrasound-mediated gene delivery: preparation and in vitro characterization. Int J Nanomedicine **7:**3309-3318.

19. Collis J, Manasseh R, Liovic P, Tho P, Ooi A, Petkovic-Duran K, Zhu Y 2010 Cavitation microstreaming and stress fields created by microbubbles. Ultrasonics **50:**273-279.

20. Gao Z, Kennedy AM, Christensen DA, Rapoport NY 2008 Drug-Loaded Nano/Microbubbles for Combining Ultrasonography and Targeted Chemotherapy. Ultrasonics **48:**260-270.

21. Horie S, Watanabe Y, Ono M, Mori S, Kodama T 2011 Evaluation of antitumor effects following tumor necrosis factor-α gene delivery using nanobubbles and ultrasound. Cancer Sci **102:**2082-2089.

22. Karshafian R, Bevan PD, Williams R, Samac S, Burns PN 2009. Sonoporation by ultrasound-activated microbubble contrast agents: effect of acoustic exposure parameters on cell membrane permeability and cell viability. Ultrasound Med Biol **35:**847-860.

23. Wang Y, Li X, Zhou Y, Huang P, Xu Y 2010. Preparation of nanobubbles for ultrasound imaging and intracellular drug delivery. Int J Pharm **384:**148-153.

24. Jocham D, Chaussy C, Schmiedt E 1986. Extracorporeal shock wave lithotripsy. Urol Int **41:**357-368.

25. Frairia R, Catalano MG, Fortunati N, Fazzari A, Raineri M, Berta L 2003 High energy shock waves (HESW) enhance paclitaxel cytotoxicity in MCF-7 cells. Breast Cancer Res Treat **81:**11-19.

26. Kodama T, Doukas AG, Hamblin MR 2002 Shock wave-mediated molecular delivery into cells. Biochim Biophys Acta **1542:**186-194.

27. Lauer U, Bürgelt E, Squire Z, Messmer K, Hofschneider PH, Gregor M, Delius M 1997 Shock wave permeabilization as a new gene transfer method. Gene Ther **4:**710-715.

28. Catalano MG, Costantino L, Fortunati N, Bosco O, Pugliese M, Boccuzzi G, Berta L, Frairia R 2007 High energy shock waves activate 5'-aminolevulinic Acid and increase permeability to Paclitaxel: antitumor effects of a new combined treatment on anaplastic thyroid cancer cells. Thyroid **17:**91-99.

29. Canaparo R, Serpe L, Zara GP, Chiarle R, Berta L, Frairia R 2008 High energy shock waves (ESW) increase paclitaxel efficacy in a syngeneic model of breast cancer. Technol Cancer Res Treat **7:**117-124.

30. Palmero A, Berger M, Venturi C, Ferrero I, Rustichelli D, Berta L, Frairia R, Madon E, Fagioli F 2006 High energy shock waves enhance the cytotoxic effect of doxorubicin and methotrexate to human osteosarcoma cell lines. Oncol Rep **15:**267-273.

31. Bekeredjian R, Bohris C, Hansen A, Katus HA, Kuecherer HF, Hardt SE 2007 Impact of Microbubbles on Shock Wave-Mediated DNA Uptake in Cells In Vitro. Ultrasound Med Biol **33:**743-750.

32. Ogden JA, Alvarez RG, Levitt R, Marlow M 2001 Shockwave therapy (Orthotripsy®) in musculoskeletal disorders. Clin Orthop Relat Res **387:**22-40.

33. Swenson CE, Bolcsak LE, Batist G, Guthrie TH Jr, Tkaczuk KH, Boxenbaum H, Welles L, Chow SC, Bhamra R, Chaikin P 2003 Pharmacokinetics of doxorubicin administered iv as Myocet (TLC D-99, liposome-encapsulated doxorubicin citrate) compared with conventional doxorubicin when given in combination with cyclophosphamide in patients with metastatic breast cancer. Anticancer Drugs **14:**239-246.

34. Ricarte-Filho JC, Ryder M, Chitale DA, Rivera M, Heguy A, Ladanyi M, Janakiraman M, Solit D, Knauf JA, Tuttle RM, Ghossein RA, Fagin JA 2009 Mutational profile of advanced primary and metastatic radioactive iodine-

refractory thyroid cancers reveals distinct pathogenetic roles for BRAF, PIK3CA, and AKT1. Cancer Res **69:**4885-4893.

35. Kunstman JW, Juhlin CC, Goh G, Brown TC, Stenman A, Healy JM, Rubinstein JC, Choi M, Kiss N, Nelson-Williams C, Mane S, Rimm DL, Prasad ML, Höög A, Zedenius J, Larsson C, Korah R, Lifton RP, Carling T 2015 Characterization of the mutational landscape of anaplastic thyroid cancer via whole-exome sequencing. Hum Mol Genet **24:**2318-2329.

36. Nehs MA, Nagarkatti S, Nucera C, Hodin RA, Parangi S 2010 Thyroidectomy with neoadjuvant PLX4720 extends survival and decreases tumor burden in an orthotopic mouse model of anaplastic thyroid cancer. Surgery **148:**1154-1162.

37. Radhakrishnan SK, Bhat UG, Hughes DE, Wang IC, Costa RH, Gartel AL 2006 Identification of a chemical inhibitor of the oncogenic transcription factor forkhead box M. Cancer Res **66:**9731-9735.

38. Kwok JM, Myatt SS, Marson CM, Coombes RC, Constantinidou D, Lam EW 2008 Thiostrepton selectively targets breast cancer cells through inhibition of FOXM1 expression. Mol Cancer Ther **7:**2022-2032.

39. Bellelli R, Castellone MD, Garcia-Rostan G, Ugolini C, Nucera C, Sadow PM, Nappi TC, Salerno P, Cantisani MC, Basolo F, Gago TA, Salvatore G, Santoro M 2012 FOXM1 is a molecular determinant of the mitogenic and invasive phenotype of anaplastic thyroid carcinoma. Endocr Relat Cancer **19:**695-710.

40. Catalano MG, Pugliese M, Gargantini E, Grange C, Bussolati B, Asioli S, Bosco O, Poli R, Compagnone A, Bandino A, Mainini F, Fortunati N, Boccuzzi G

2012 Cytotoxic activity of the histone deacetylase inhibitor panobinostat (LBH589) in anaplastic thyroid cancer in vitro and in vivo. Int J Cancer **130:**694-704.

41. Catalano MG, Fortunati N, Pugliese M, Marano F, Ortoleva L, Poli R, Asioli S, Bandino A, Palestini N, Grange C, Bussolati B, Boccuzzi G. 2012 Histone deacetylase inhibition modulates E-cadherin expression and suppresses migration and invasion of anaplastic thyroid cancer cells. J Clin Endocrinol 97:E1150-1159.

42. Pugliese M, Fortunati N, Germano A, Asioli S, Marano F, Palestini N, Frairia R, Boccuzzi G, Catalano MG 2013 Histone deacetylase inhibition affects sodium iodide symporter expression and induces 131I cytotoxicity in anaplastic thyroid cancer cells. Thyroid **23:**838-846.

43. Hilmer SN, Cogger VC, Muller M, Le Couteur DG 2004 The hepatic pharmacokinetics of doxorubicin and liposomal doxorubicin. Drug Metab Dispos **32:**794-799.

44. Son YJ, Jang JS, Cho YW, Chung H, Park RW, Kwon IC, Kim IS, Park JY, Seo SB, Park CR, Jeong SY 2003 Biodistribution and anti-tumor efficacy of doxorubicin loaded glycol-chitosan nanoaggregates by EPR effect. J Control Release **91:**135-145.

45. Cho YW, Park SA, Han TH, Son DH, Park JS, Oh SJ, Moon DH, Cho KJ, Ahn CH, Byun Y, Kim IS, Kwon IC, Kim SY 2007 In vivo tumor targeting and

radionuclide imaging with self-assembled nanoparticles: mechanisms key factors and their implications. Biomaterials **28:**1236-1247.

46. Saravanakumar G, Min KH, Min DS, Kim AY, Lee CM, Cho YW, Lee SC, Kim K, Jeong SY, Park K, Park JH, Kwon IC 2009 Hydrotropic oligomer-conjugated glycol chitosan as a carrier of paclitaxel: synthesis characterization and in vivo biodistribution. J Control Release **140:**210-217.

47. Hwang HY, Kim IS, Kwon IC, Kim YH 2008 Tumor targetability and antitumor effect of docetaxel-loaded hydrophobically modified glycol chitosan nanoparticles. J Control Release **128:**23-31.

48. Hyung Park J, Kwon S, Lee M, Chung H, Kim JH, Kim YS, Park RW, Kim IS, Bong Seo S, Kwon IC, Young Jeong S 2006 Self-assembled nanoparticles based on glycol chitosan bearing hydrophobic moieties as carriers for doxorubicin: in vivo biodistribution and anti-tumor activity. Biomaterials **27:**119-126.

49. Cavalli R, Argenziano M, Vigna E, Giustetto P, Torres E, Aime S, Terreno E 2015 Preparation and in vitro characterization of chitosan nanobubbles as theranostic agents. Colloids Surf B Biointerfaces **129:**39-46.

50. Lin SF, Lin JD, Chou TC, Huang YY, Wong RJ 2013 Utility of a histone deacetylase inhibitor (PXD101) for thyroid cancer treatment. PLoS One **8:**e77684.

51. Catalano MG, Fortunati N, Pugliese M, Poli R, Bosco O, Mastrocola R, Aragno M, Boccuzzi G 2006 Valproic acid a histone deacetylase inhibitor enhances

sensitivity to doxorubicin in anaplastic thyroid cancer cells. J Endocrinol **191:**465-472.

52. Yu Y, Chen CK, Law WC, Weinheimer E, Sengupta S, Prasad PN, Cheng C 2014 Polylactide-graft-doxorubicin nanoparticles with precisely controlled drug loading for pH-triggered drug delivery. Biomacromolecule **15:**524-532.

53. Nasrollahi Z, Mohammadi SR, Mollarazi E, Yadegari MH, Hassan ZM, Talaei F, Dinarvand R, Akbari H, Atyabi F 2015 Functionalized nanoscale β-13-glucan to improve Her2+ breast cancer therapy: In vitro and in vivo study. J Control Release **202:**49-56.

54. Yu J, Xie X, Wu J, Liu Y, Liu P, Xu X, Yu H, Lu L, Che X 2013 Folic acid conjugated glycol chitosan micelles for targeted delivery of doxorubicin: preparation and preliminary evaluation in vitro. J Biomater Sci Polym Ed **24:**606-620.

55. Golla K, Bhaskar C, Ahmed F, Kondapi AK 2013 A target-specific oral formulation of Doxorubicin-protein nanoparticles: efficacy and safety in hepatocellular cancer. J Cancer **4:**644-652.

56. Tacar O, Sriamornsak P, Dass CR 2013 Doxorubicin: an update on anticancer molecular action toxicity and novel drug delivery systems. J Pharm Pharmacol 65:157-170.

57. Tewey KM, Rowe TC, Yang L, Halligan BD, Liu LF 1984 Adriamycin-induced DNA damage mediated by mammalian DNA topoisomerase II. Science **226:**466-468.

58. Nielsen D, Maare C, Skovsgaard T 1996 Cellular resistance to anthracyclines. Gen Pharmacol. **27:**251-255.

59. Lothstein L, Israel M, Sweatman TW 2001 Anthracycline drug targeting: cytoplasmic versus nuclear--a fork in the road. Drug Resist Updat **4:**169-177.

60. Lei M, Ma M, Pang X, Tan F, Li N 2015 A dual pH/thermal responsive nanocarrier for combined chemo-thermotherapy based on a copper-doxorubicin complex and gold nanorods. Nanoscale **7:**15999-16011.

61. Li J, Yang H, Zhang Y, Jiang X, Guo Y, An S, Ma H, He X, Jiang C 2015 Choline Derivate-Modified Doxorubicin Loaded Micelle for Glioma Therapy. ACS Appl Mater Interfaces **7:**21589-21601.

62. Alibolandi M, Sadeghi F, Abnous K, Atyabi F, Ramezani M, Hadizadeh F 2015 The chemotherapeutic potential of doxorubicin-loaded PEG-b-PLGA nanopolymersomes in mouse breast cancer model. Eur J Pharm Biopharm. **94:**521-31.

63. Diederich CJ, Hynynen K 1999 Ultrasound technology for hyperthermia. Ultrasound Med Biol **25:**871-887.

FIGURE LEGENDS

FIG. 1. Characterization of NBs. TEM image of glycol chitosan NBs (scale bar 250 nm) (A). *In vitro* release kinetics of doxorubicin from doxorubicin-loaded glycol chitosan NBs with or without ESWs treatment (500 pulses, 0.59 mJ/mm^2) (B). Data are shown as percentage of released doxorubicin vs time 0.

FIG. 2. Effect of ESWs and empty NBs on cell viability. Growth curve of CAL-62 (A) and 8305C (B) cells after treatment with ESWs (500 pulses at 0.59 mJ/mm^2) expressed as viability ratio *vs* time 0. Viability of CAL-62 (C) and 8305C (D) cells treated for 72 hours with empty NBs (0.9-5.4 x 10^6 NBs/ml). Viability of CAL-62 (E) and 8305C (F) cells treated with empty NBs (0.9-5.4 x 10^6 NBs/ml) in combination with ESWs. Viability is expressed as ratio between absorbance of treated cells *vs* absorbance of untreated cells (abs=0.267 ± 0.005 for CAL-62; abs=0.523 ± 0.026 for 8305C).

FIG. 3. Glycol chitosan NB entrance. Cytofluorimetric analysis of CAL-62 (A) and 8305C (B) cells treated for 24 hours with 6-coumarin-labelled glycol chitosan NBs (0.9-5.4 x 10^6 NBs/ml) expressed as Mean Fluorescence Intensity (MFI). Significance *vs* untreated cells (0): $p<0.01$ (**); $p<0.001$ (***). Photos by fluorescence microscope of CAL-62 (C) and 8305C (D) cells treated with 6-coumarin-labelled glycol chitosan NBs at 0.9 and 1.8 x 10^6 NBs/ml. Pictures were taken at 200 x final magnification (scale bar: 100 µm). In the right inset a 400 x final magnification detail is reported (scale bar: 50 µm). The images are representative of three independent experiments.

FIG. 4. Cytotoxicity of doxorubicin-loaded NBs. Cytotoxic effects of doxorubicin (A, CAL-62; B, 8305C); doxorubicin + ESWs (C, CAL-62; D, 8305C); doxorubicin-loaded glycol chitosan NBs (E, CAL-62; F, 8305C); doxorubicin-loaded glycol chitosan NBs +

ESWs (G, CAL-62; H, 8305C) evaluated up to 48 hours. ESW treatment was performed at 500 pulses at 0.59 mJ/mm^2. Viability is expressed as ratio between absorbance at 24 and 48 hours *vs* absorbance at time 0 (abs=0.043 ± 0.004 for CAL-62; abs=0.276 ± 0.036 for 8305C). Significance *vs* Basal: $p<0.05$ (*); $p<0.01$ (**); $p<0.001$ (***).

FIG. 5. Effect of NBs on rat H9C2 cardiomyocytes. Viability of H9C2 cells after 72 hours of treatment with empty NBs (0.9-5.4 x 10^6 NBs/ml) (A). Cytofluorimetric analysis of H9C2 cells treated with 6-coumarin-labelled glycol chitosan NBs at 0.9-5.4 x 10^6 NBs/ml (B) expressed as Mean Fluorescence Intensity (MFI). Significance *vs* untreated cells (0): $p<0.01$ (**); $p<0.001$ (***). Viability of H9C2 treated with free doxorubicin (C) or doxorubicin-loaded NBs (D) (0.25-3 μM). Viability is expressed as ratio between absorbance of treated cells *vs* absorbance of untreated cells (Basal; abs= 0.099 ± 0.017). Significance *vs* Basal: $p<0.01$ (**); $p<0.001$ (***).

FIG. 6. Effects of ESWs on NBs. Pictures of CAL-62 (upper panels) and 8305C (lower panels) cells treated with FITC-labelled doxorubicin-loaded glycol chitosan NBs, in the presence (d-f; d'-f') or absence (a-c; a'-c') of ESWs (500 pulses, 0.59 mJ/mm^2). Green fluorescence of FITC (a, d, a', d'), red fluorescence of doxorubicin (b, e, b', e') and merge (c, f, c', f') photos were taken at 200 x final magnification (scale bar: 100 μm). In the right inset an enlarged detail of the overlaid pictures is shown. The images are representative of three independent experiments.

FIG. 7. Intracellular content of doxorubicin. Doxorubicin content was measured in whole cell lysate (A) and in cytosolic/nuclear compartments (B) at 24 hours after treatment with free doxorubicin or doxorubicin-loaded NBs in the presence or absence of ESW treatment (500 pulses, 0.59 mJ/mm^2). Drug amount was expressed as ng/10^6 cells. Significance, in whole cell lysate (A): doxorubicin + ESWs *vs* doxorubicin,

$p<0.01$ (**); doxorubicin-loaded NBs *vs* doxorubicin, and doxorubicin-loaded NBs + ESWs *vs* doxorubicin: $p<0.001$ (***). Significance, in cytosolic/nuclear compartments (B): doxorubicin + ESWs *vs* doxorubicin, and doxorubicin-loaded NBs + ESWs *vs* doxorubicin-loaded NBs: $p<0.01$ (°°); doxorubicin-loaded NBs *vs* doxorubicin, and doxorubicin-loaded NBs + ESWs *vs* doxorubicin: $p<0.001$ (###).

TABLE 1. Physic-chemical characteristics of NB formulations

	Glycol chitosan NBs (empty)	**Doxorubicin-loaded glycol chitosan NBs**
Average diameters ± SD (nm)	465.5 ± 16.3	480.2 ± 18.5
PDI	0.19 ± 0.01	0.20 ± 0.02
ζ-Potential ± SD (mV)	30.5 ± 2.36	29.6 ± 3.94

TABLE 2. GI_{50} was calculated in ATC cells for doxorubicin and doxorubicin-loaded glycol chitosan NBs in the presence or absence of ESWs. Significance: doxorubicin + ESWs *vs* doxorubicin, $p<0.05$ (*) in both cell lines; doxorubicin-loaded NBs *vs* doxorubicin: $p<0.001$(***) in CAL-62, and $p<0.05$ (*) in 8305C; doxorubicin-loaded NBs + ESWs *vs* doxorubicin: $p<0.001$(***) in both cell lines; doxorubicin + empty NBs + ESWs *vs* doxorubicin: $p<0.01$(**) in CAL-62; doxorubicin-loaded NBs + ESWs *vs* doxorubicin-loaded NBs: $p<0.05$ (°) in CAL-62, and $p<0.01$(°°) in 8305C.

	GI_{50} (μM)[i]			
	CAL-62		**8305C**	
Treatments	***NO ESWs***	***ESWs***	***NO ESWs***	***ESWs***
Doxorubicin	1.57 ± 0.03	1.33 ± 0.08 (*)	3.93 ± 0.09	3.17 ± 0.04 (*)
Doxorubicin-loaded glycol chitosan NBs	1.13 ± 0.03 (***)	0.95 ± 0.03 (***) (°)	2.98 ± 0.08 (*)	2.12 ± 0.09 (***) (°°)
Doxorubicin + empty NBs	-	1.26 ± 0.01 (**)	-	-

[i] ESWs enhanced doxorubicin-loaded NB cytotoxicity decreasing the drug GI_{50} of 40 % in CAL-62 and 46 % in 8305C cells, respectively.

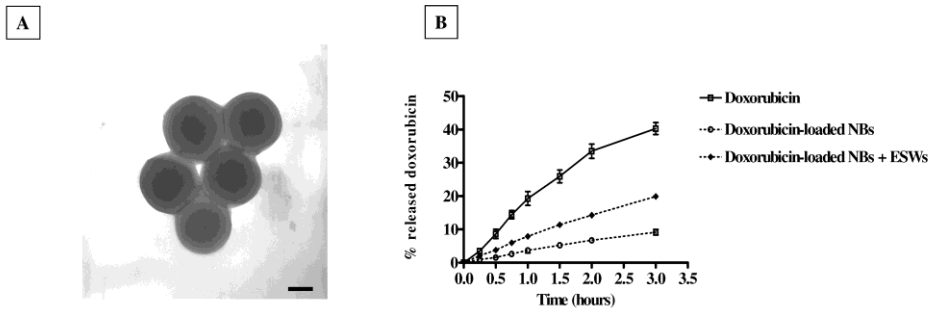
A
B
% released doxorubicin
50
40
30
20
10
0
0.0 0.5 1.0 1.5 2.0 2.5 3.0 3.5
Time (hours)
Doxorubicin
Doxorubicin-loaded NBs
Doxorubicin-loaded NBs + ESWs

FIG. 1

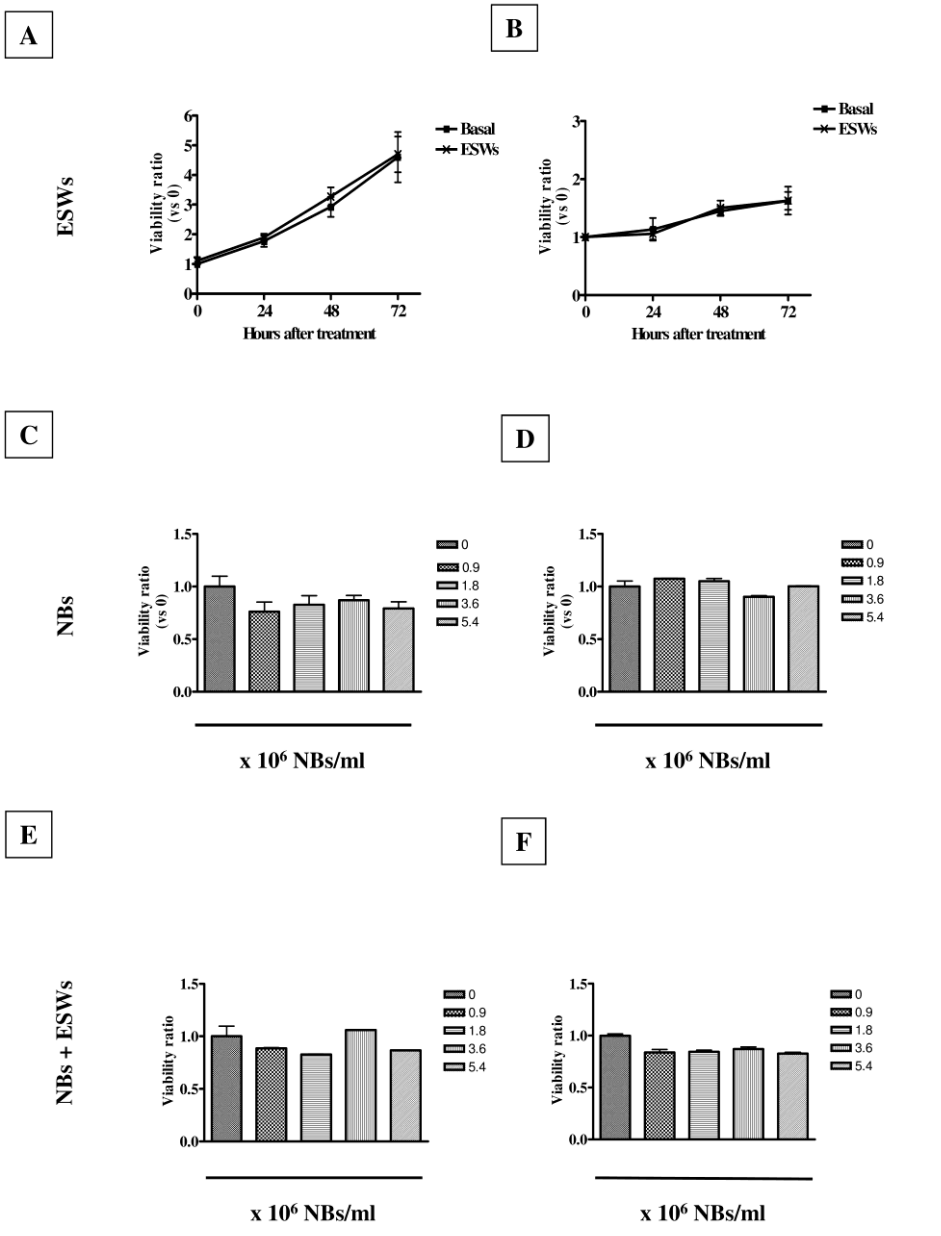
A
B
ESWs
Viability ratio (vs 0)
Hours after treatment
Basal
ESWs
C
D
NBs
0
0.9
1.8
3.6
5.4
x 10⁶ NBs/ml
E
F
NBs + ESWs

FIG. 2

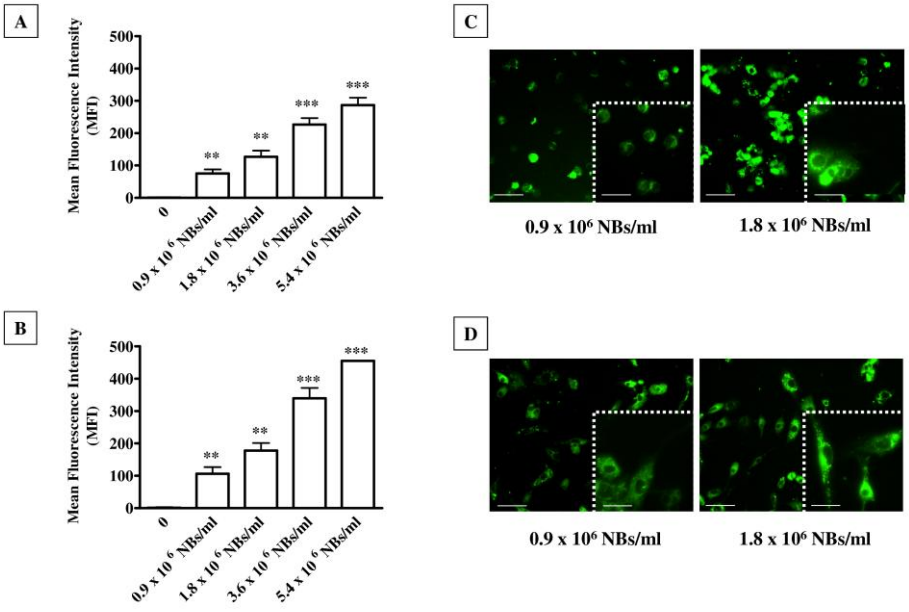
A
Mean Fluorescence Intensity (MFI)
500
400
300
200
100
0
**
**
***
***
0
0.9 x 10 6 NBs/ml
1.8 x 10 6 NBs/ml
3.6 x 10 6 NBs/ml
5.4 x 10 6 NBs/ml
C
0.9 x 10⁶ NBs/ml
1.8 x 10⁶ NBs/ml
B
Mean Fluorescence Intensity (MFI)
500
400
300
200
100
0
**
**
***
***
0
0.9 x 10 6 NBs/ml
1.8 x 10 6 NBs/ml
3.6 x 10 6 NBs/ml
5.4 x 10 6 NBs/ml
D
0.9 x 10⁶ NBs/ml
1.8 x 10⁶ NBs/ml

FIG. 3

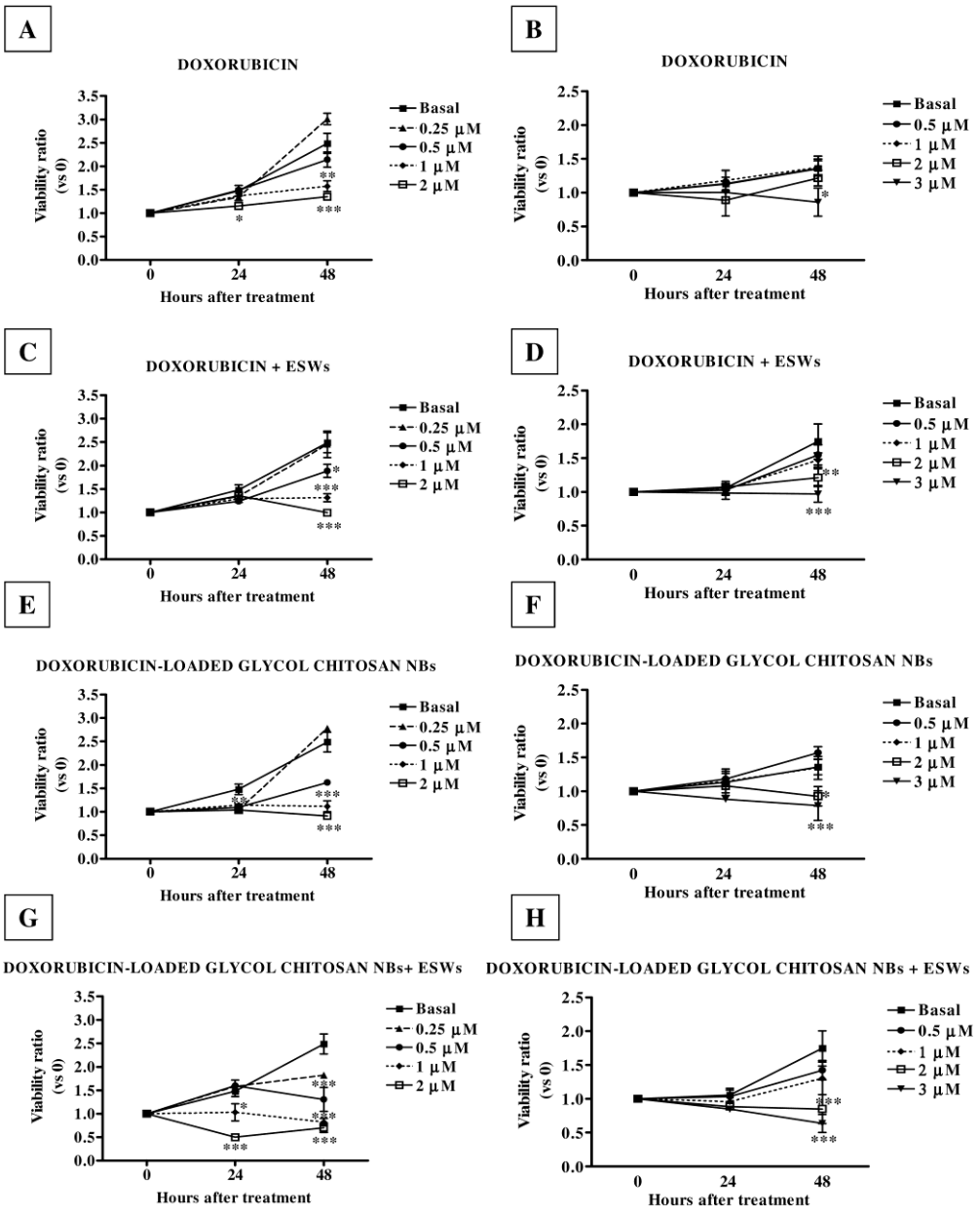
A
DOXORUBICIN
Viability ratio (vs 0)
Hours after treatment
Basal
0.25 µM
0.5 µM
1 µM
2 µM
B
DOXORUBICIN
Viability ratio (vs 0)
Hours after treatment
Basal
0.5 µM
1 µM
2 µM
3 µM
C
DOXORUBICIN + ESWs
Viability ratio (vs 0)
Hours after treatment
Basal
0.25 µM
0.5 µM
1 µM
2 µM
D
DOXORUBICIN + ESWs
Viability ratio (vs 0)
Hours after treatment
Basal
0.5 µM
1 µM
2 µM
3 µM
E
DOXORUBICIN-LOADED GLYCOL CHITOSAN NBs
Viability ratio (vs 0)
Hours after treatment
Basal
0.25 µM
0.5 µM
1 µM
2 µM
F
DOXORUBICIN-LOADED GLYCOL CHITOSAN NBs
Viability ratio (vs 0)
Hours after treatment
Basal
0.5 µM
1 µM
2 µM
3 µM
G
DOXORUBICIN-LOADED GLYCOL CHITOSAN NBs+ ESWs
Viability ratio (vs 0)
Hours after treatment
Basal
0.25 µM
0.5 µM
1 µM
2 µM
H
DOXORUBICIN-LOADED GLYCOL CHITOSAN NBs + ESWs
Viability ratio (vs 0)
Hours after treatment
Basal
0.5 µM
1 µM
2 µM
3 µM

FIG. 4

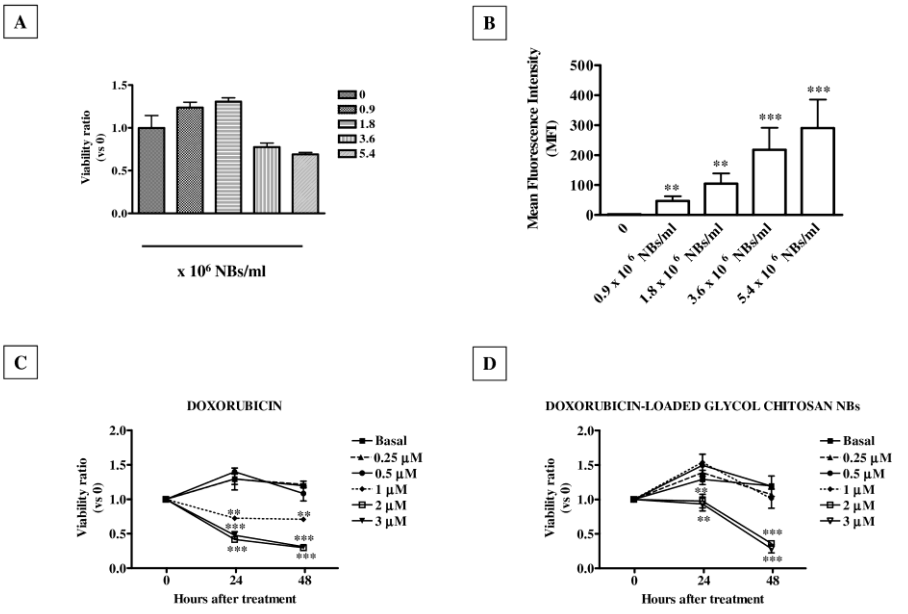
A
Viability ratio (vs 0)
0
0.9
1.8
3.6
5.4
x 10⁶ NBs/ml
B
Mean Fluorescence Intensity (MFI)
0
0.9 x 10⁶ NBs/ml
1.8 x 10⁶ NBs/ml
3.6 x 10⁶ NBs/ml
5.4 x 10⁶ NBs/ml
C
DOXORUBICIN
Viability ratio (vs 0)
Basal
0.25 µM
0.5 µM
1 µM
2 µM
3 µM
Hours after treatment
D
DOXORUBICIN-LOADED GLYCOL CHITOSAN NBs
Viability ratio (vs 0)
Basal
0.25 µM
0.5 µM
1 µM
2 µM
3 µM
Hours after treatment

FIG. 5

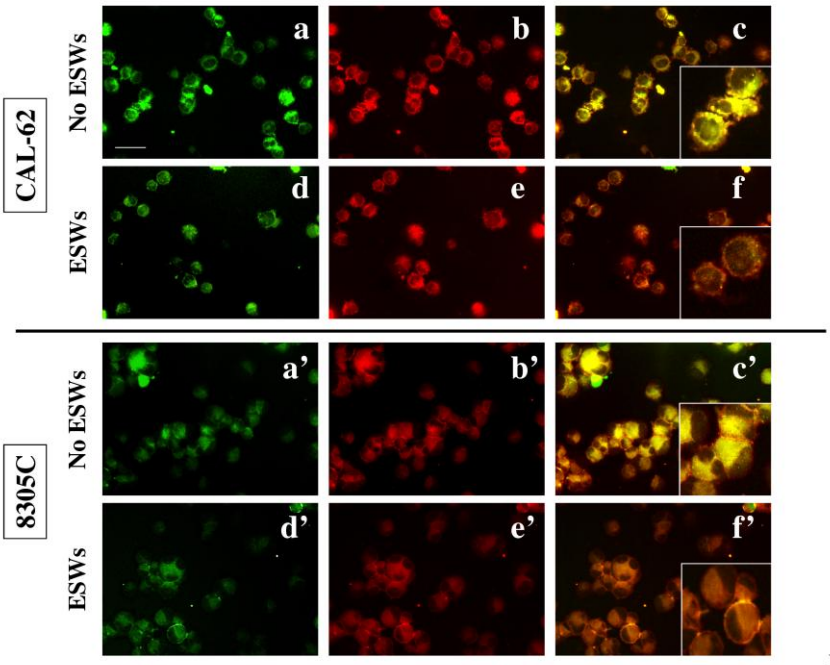
CAL-62
No ESWs
ESWs
a
b
c
d
e
f
8305C
No ESWs
ESWs
a'
b'
c'
d'
e'
f'

FIG. 6

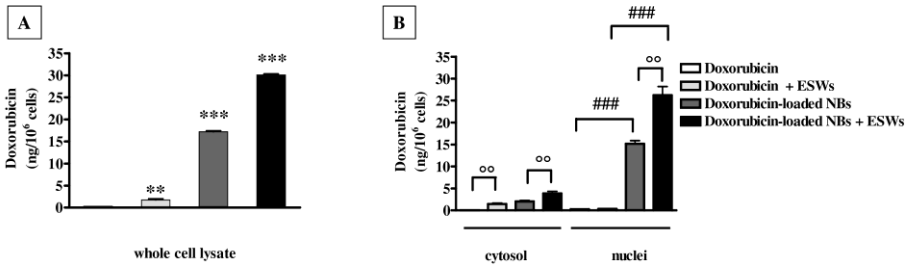
A
Doxorubicin (ng/10^6 cells)
35
30
25
20
15
10
5
0
**
***
***
whole cell lysate
B
###
°°
°°
###
°°
Doxorubicin
Doxorubicin + ESWs
Doxorubicin-loaded NBs
Doxorubicin-loaded NBs + ESWs
cytosol
nuclei

FIG. 7